

## RESEARCH REPORT

# A link between planar polarity and staircase-like bundle architecture in hair cells

Basile Tarchini<sup>1,2,3,4,\*</sup>, Abigail L. D. Tadenev<sup>1</sup>, Nicholas Devanney<sup>1</sup> and Michel Cayouette<sup>4,5,6,\*</sup>

## ABSTRACT

Sensory perception in the inner ear relies on the hair bundle, the highly polarized brush of movement detectors that crowns hair cells. We previously showed that, in the mouse cochlea, the edge of the forming bundle is defined by the ‘bare zone’, a microvilli-free sub-region of apical membrane specified by the Insc-LGN-G $\alpha$ i protein complex. We now report that LGN and G $\alpha$ i also occupy the very tip of stereocilia that directly abut the bare zone. We demonstrate that LGN and G $\alpha$ i are both essential for promoting the elongation and differential identity of stereocilia across rows. Interestingly, we also reveal that total LGN-G $\alpha$ i protein amounts are actively balanced between the bare zone and stereocilia tips, suggesting that early planar asymmetry of protein enrichment at the bare zone confers adjacent stereocilia their tallest identity. We propose that LGN and G $\alpha$ i participate in a long-inferred signal that originates outside the bundle to model its staircase-like architecture, a property that is essential for direction sensitivity to mechanical deflection and hearing.

**KEY WORDS:** Hair cell, Hair bundle, Stereocilia, Staircase-like organization, LGN/Gpsm2, G $\alpha$ i, Mouse

## INTRODUCTION

Spearheading sensory perception in the inner ear, epithelial hair cells (HCs) transform sound waves, gravity or head movements into electrical impulses that are relayed to the brain by peripheral neurons. Hair bundle deflection exerts force on molecular tip-links that connect neighboring shorter and taller stereocilia across rows, which activates the transduction machinery located at the base of each link (Zhao and Müller, 2015). HCs are receptive to bundle displacements along a single planar axis that is indicated by the direction of the gradient of stereocilia height (Pickles et al., 1984; Shotwell et al., 1981). How the bundle adopts its staircase pattern, however, remains largely unclear. Resident bundle proteins such as Myo15a and Myo3a, and their cargo delivered to stereocilia tips, are required to various extents for graded heights and concurrent graded amounts of some proteins at tips across rows (Belyantseva et al., 2003, 2005; Ebrahim et al., 2016; Lelli et al., 2016; Manor et al., 2011; Mburu et al., 2003; Probst et al., 1998; Salles et al., 2009).

<sup>1</sup>The Jackson Laboratory, Bar Harbor, ME 04609, USA. <sup>2</sup>Department of Medicine, Tufts University, Boston, MA 02111, USA. <sup>3</sup>Graduate School of Biomedical Science and Engineering (GSBSE), University of Maine, Orono, ME 04469, USA. <sup>4</sup>Cellular Neurobiology Research Unit, Institut de recherches cliniques de Montréal (IRCM), Montréal, Québec, Canada H2W 1R7. <sup>5</sup>Department of Medicine, Université de Montréal, Montréal, Québec, Canada H3T 1J4. <sup>6</sup>Department of Anatomy and Cell Biology, and Division of Experimental Medicine, McGill University, Montréal, Québec, Canada H3A 0G4.

\*Authors for correspondence (basile.tarchini@jax.org; michel.cayouette@ircm.qc.ca)

 B.T., 0000-0003-2708-6273; M.C., 0000-0003-4655-9048

Received 25 April 2016; Accepted 14 September 2016

However, the mechanisms that instruct morphological and molecular asymmetry across the bundle remain unknown. External cues, including a role for the extracellular matrix or the kinocilium, have been proposed but not experimentally validated (Manor and Kachar, 2008).

Tissue and cell polarization during early development lay the structural foundations required for sensory function. Before a marked staircase pattern and tip-links arise postnatally in the mouse cochlea, ‘core’ planar cell polarity (PCP) proteins that are asymmetrically enriched at cell-cell junctions ensure uniform bundle orientation across HCs (May-Simera and Kelley, 2012). Furthermore, recent studies have clarified that planar asymmetry of the cytoskeleton in each HC (which is manifested, for example, by the V-shaped or semi-circular edge of the bundle and the off-center position of the kinocilium) depends on ciliary proteins, small GTPases and the Insc-LGN-G $\alpha$ i complex (Bhonker et al., 2016; Ezan et al., 2013; Grimsley-Myers et al., 2009; Jones et al., 2008; Sipe and Lu, 2011; Tarchini et al., 2013). As the staircase pattern of the hair bundle is effectively a planar asymmetry in stereocilia height, we investigate here whether cell-intrinsic planar polarity signals could participate in its establishment. We show that following their planar polarized enrichment at the ‘bare zone’, which is the smooth apical sub-region that defines the lateral edge of the bundle (Tarchini et al., 2013), LGN (Gpsm2) and G $\alpha$ i become specifically enriched at the tips of adjacent stereocilia that will form the tallest row. Stunted postnatal stereocilia and lack of differential identity across rows in absence of LGN and G $\alpha$ i function suggest a model whereby planar polarity information in the flat region of the apical membrane is used to establish differential stereocilia identity across the bundle.

## RESULTS AND DISCUSSION

### LGN and G $\alpha$ i colocalize at the tips of stereocilia in the first row

Insc-LGN-G $\alpha$ i are planar polarized in murine cochlear post-mitotic HCs from embryonic day (E) 15.0 (Bhonker et al., 2016; Ezan et al., 2013; Tarchini et al., 2013), labeling and expanding the bare zone (Tarchini et al., 2013). At E16.5, we found that LGN and G $\alpha$ i become enriched in a second apical compartment: the tips of developing stereocilia in inner hair cells (IHCs) (Fig. 1A; data not shown). At birth, in both IHCs and outer hair cells (OHCs), LGN and G $\alpha$ i, but not Insc, are detected at the distal tip of stereocilia adjacent to the bare zone (Fig. 1B). Although initially restricted to central stereocilia in the bundle, LGN-G $\alpha$ i spread to encompass all stereocilia in the first row (Fig. 1C). Stereocilia enrichment becomes more prominent after birth, whereas protein accumulation at the bare zone, which dominates during embryogenesis, concomitantly decreases (Fig. 1D). LGN-G $\alpha$ i amounts at the tips are initially comparable in IHCs and OHCs, but decrease during bundle maturation in OHCs (Fig. S1A). LGN-G $\alpha$ i immunostaining signal extends distally beyond F-actin in the tallest row, but is undetectable in shorter rows (Fig. 1E,F; Fig.

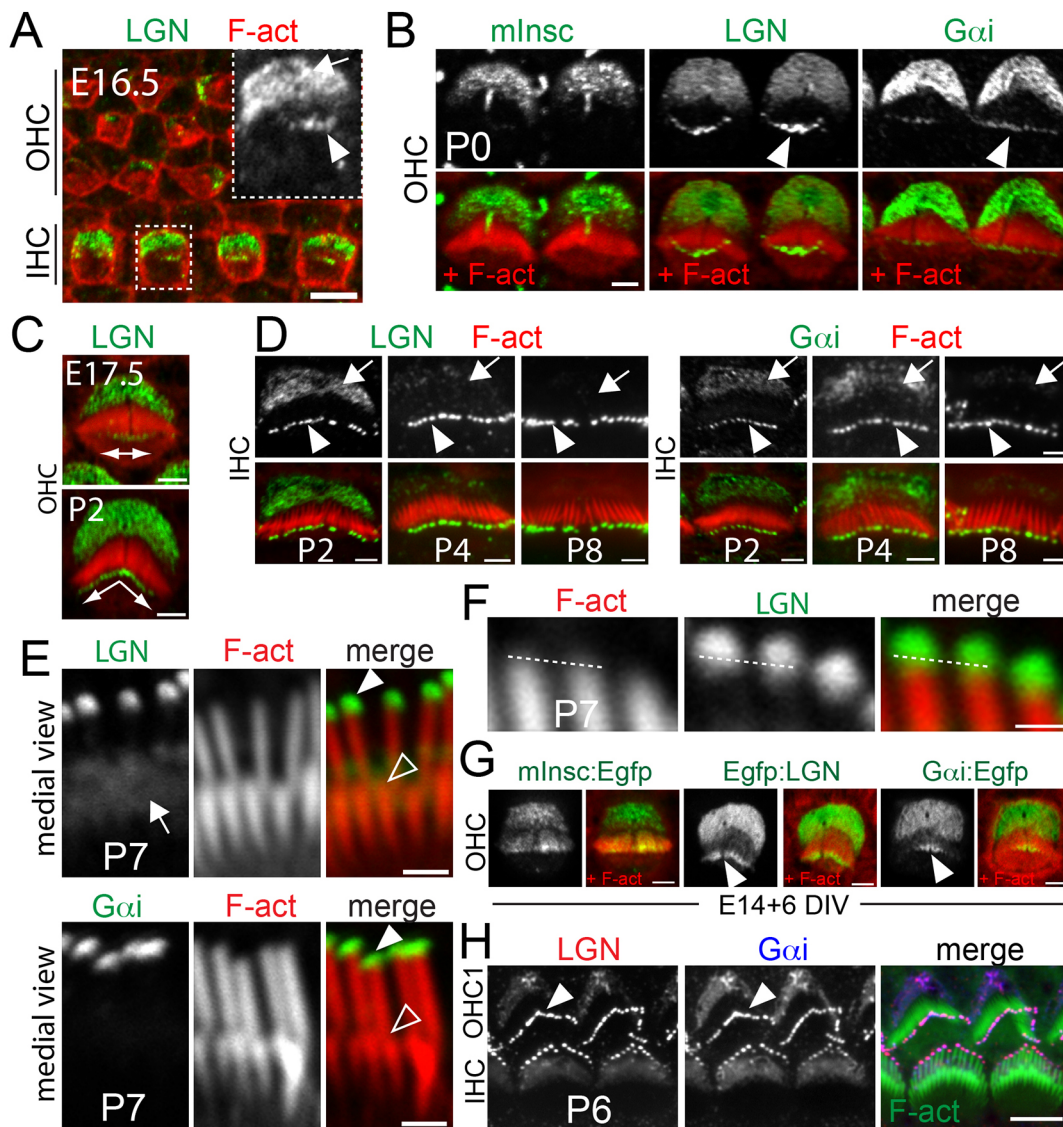


**Fig. 1. LGN and  $G\alpha i$ , but not *Insc*, localize at the distal tip of stereocilia in the tallest row.** (A) LGN immunostaining at E16.5 (one turn position). Inset: LGN channel from the boxed IHC region. (B) *Insc*, LGN and  $G\alpha i$  immunostaining at P0 (base). (C) LGN at E17.5 and P2. Stereocilia tip enrichment (double-headed arrow) is initially restricted to central stereocilia, but spreads peripherally with time. (D) LGN and  $G\alpha i$  in IHCs at P2, P4 and P8. Bare zone localization decreases with time. (E) Medial view of LGN and  $G\alpha i$  in P7 IHC bundles. No protein enrichment is detected at tips in the second row. See Fig. S1B for a lateral side view. (F) Higher magnification view of LGN at the tips. LGN extends distally beyond the F-actin core of stereocilia (broken lines). (G) Egfp-tagged LGN and  $G\alpha i$  recapitulate endogenous protein distribution, including stereocilia tips. Tagged *Insc* localizes at the bare zone and can invade the bundle, but is not specifically enriched at stereocilia tips. Cochleas were electroporated at E14.5 and cultured for 6 days. (H) Co-immunostaining for LGN and  $G\alpha i$  at P6 (one turn position). Solid arrowheads, stereocilia tips in the first row; open arrowheads, stereocilia tips in the second row; arrows, bare zone. All images are *en face* views of the apical surface of the cochlear sensory epithelium where lateral (abneural) is upwards and medial (neural) is downwards. F-actin (F-act) is labeled with phalloidin. Scale bars: 5  $\mu$ m in A,H; 2  $\mu$ m in B-E,G; 1  $\mu$ m in F.

S1B), and a similar protein distribution is observed in vestibular HCs (Fig. S1C). Importantly, LGN signal in stereocilia is absent in *Lgn* mutants (Fig. S1D), and this specific tip enrichment is recapitulated when LGN and  $G\alpha i$  proteins carrying Myc or Egfp tags are transfected into HCs in cochlear cultures (Fig. 1G; Fig. S1E). Overexpressed fusion proteins maintain specificity for the first row (Fig. S1E), suggesting that LGN- $G\alpha i$  are not able to enter shorter stereocilia located further away from the bare zone. At all stages, LGN and  $G\alpha i$  colocalize at tips in a similar way to their colocalization at the bare zone (Fig. 1H; Fig. S1E), as expected from their well-established direct binding (Du and Macara, 2004). Together, these results uncover a novel and intriguing dual subcellular LGN- $G\alpha i$  distribution in HCs that suggests a potential role in stereocilia development.

### LGN and $G\alpha i$ are required for stereocilia elongation during bundle maturation

LGN or  $G\alpha i$  inactivation leads to disorganization of stereocilia distribution at the HC apical membrane (Bhonker et al., 2016; Ezan et al., 2013; Tarchini et al., 2013), which we interpreted to be the result of defective bare zone specification and expansion (Tarchini et al., 2013). Prompted by LGN- $G\alpha i$  localization at their tips, we undertook a detailed analysis of stereocilia morphology during development. Interestingly, in *Lgn* mutants, IHC stereocilia in the first row are slightly shorter at birth (postnatal day 0, P0) (Fig. 2A-C), a phenotype that increases in severity at P6 and results in drastically stunted stereocilia at maturity (Fig. 2B,C; Fig. S3). While mature IHC stereocilia

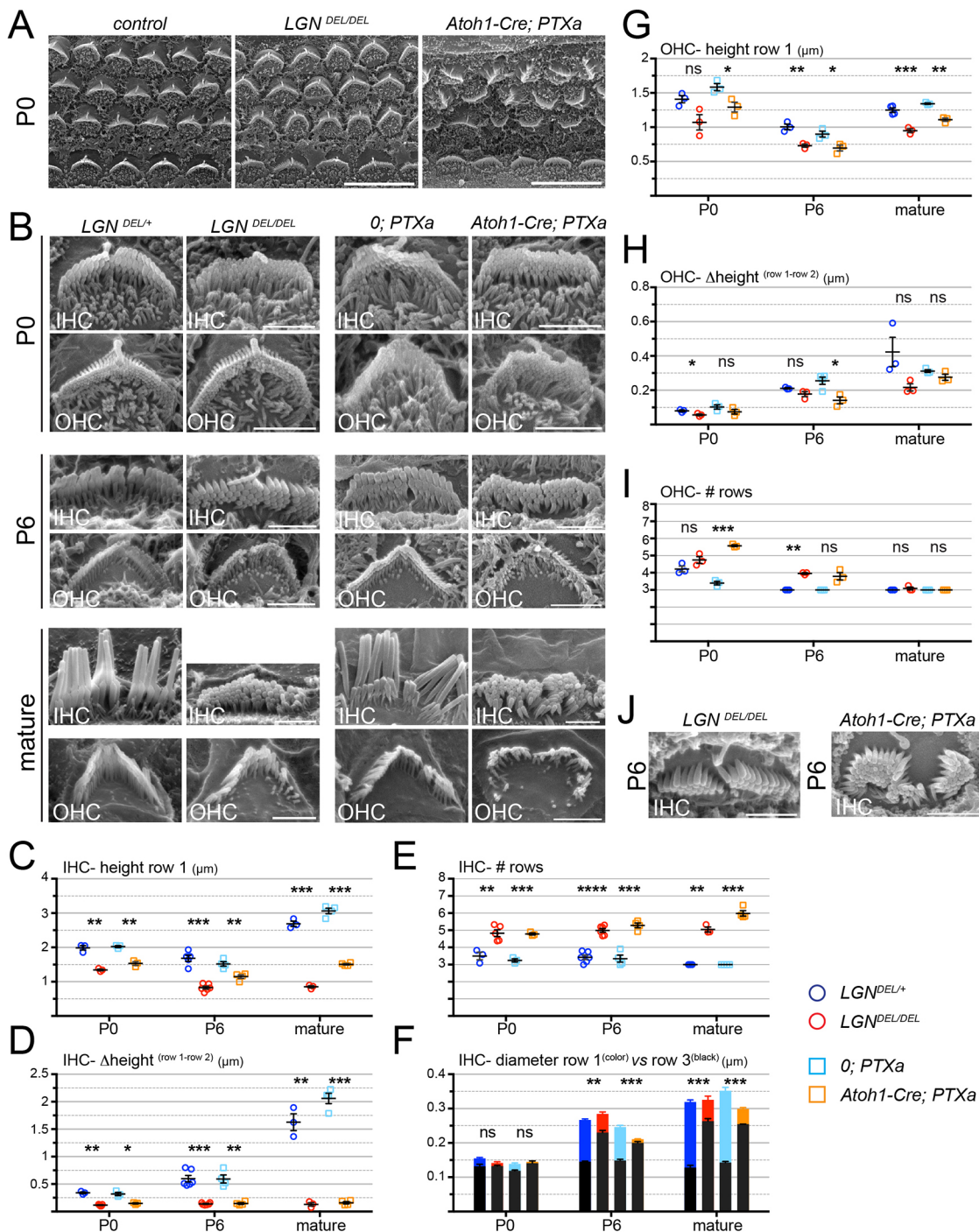


**Fig. 2. Hair bundle defects in the absence of LGN and *Gai* function.** (A) Scanning electron microscopy of the organ of Corti at P0 (half-turn) in a control ( $Lgn^{DEL/+}$ ) and in  $Lgn^{DEL/DEL}$  and  $Atoh1-Cre; PTXa$  mutants. (B) Higher magnification medial views of representative single IHCs (top) and OHCs (bottom) at P0, P6 and mature stages. Mature  $Lgn$  and  $PTXa$  samples are at P14 and P22, respectively. See lateral views in Fig. S3A. (C–F) Quantification of IHC stereocilia height in the first row (C), the height differential between the first and second row (D), the number of rows across the bundle (E), and the stereocilia thickness in the first (colored) and third (black) rows (F). (G–I) Quantification of OHC stereocilia height in the first row (G), the height differential between the first and second row (H), and the number of rows across the bundle (I). (J) Representative examples of defective stereocilia distribution in  $Lgn^{DEL/DEL}$  and  $Atoh1-Cre; PTXa$  mutants.  $0; PTXa$  controls have the  $Rosa26-stop-PTXa$  allele, but lack the  $Atoh1-Cre$  transgene. Average per animal  $\pm$  s.e.m. is plotted for  $n \geq 3$  animals. Welch's *t*-test (ns,  $P > 0.05$ ; \* $P \leq 0.05$ ; \*\* $P \leq 0.01$ ; \*\*\* $P \leq 0.001$ ; \*\*\*\* $P \leq 0.0001$ ). In F, the *t*-test reflects thickness differences in row 3. All stereocilia quantifications are detailed in Tables S1 and S2. Cochleas were analyzed halfway in the basal turn (P0, P6) and at the apical turn (mature). Scale bars: 10  $\mu\text{m}$  in A; 2  $\mu\text{m}$  in B, J.

normally form three rows of markedly different height and girth, the supernumerary rows of similar thickness and a very shallow staircase pattern in  $Lgn$  mutants suggest that the bundles remain immature (Fig. 2B,D–F).

To bypass functional redundancy between  $Gnai1$ ,  $Gnai2$  and  $Gnai3$ , we have previously analyzed transgenic fetuses expressing Pertussis toxin catalytic subunit (PTXa) in HCs (Tarchini et al., 2013). PTXa specifically ADP-ribosylates inhibitory G proteins, as

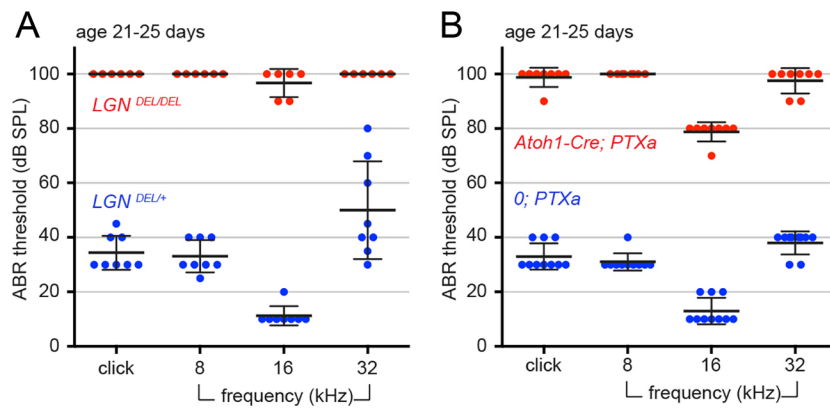


**Fig. 3. Absence of LGN and *Gai* function leads to profound deafness.** Auditory brainstem response thresholds for constitutive *Lgn* mutants (*Lgn*<sup>DEL/DEL</sup>) (A) and *Gai* inactivation in post-mitotic HCs (*Atoh1-Cre; PTXa*) (B). *Lgn*<sup>DEL/DEL</sup> ( $n=6$ ) and *Lgn*<sup>DEL/+</sup> control littermates ( $n=8$ ), *Atoh1-Cre; PTXa* ( $n=8$ ) and *0; PTXa* ( $n=10$ ) control littermates (without the *Atoh1-Cre* transgene) were tested once at P21–P25 (mean $\pm$ s.d.).

only this class of G proteins carries a conserved C-terminal cysteine target site; PTXa is routinely used to inactivate *Gai* signaling (Milligan, 1988; Wise et al., 1997). To extend this approach, we produced a stable mouse line in which PTXa expression is Cre-inducible at the *Rosa26* locus (Fig. S2A,B). Using *FoxG1-Cre* (Hébert and McConnell, 2000) to induce PTXa in early otic progenitors, we observed cochlear defects that are apparently restricted to HC apical differentiation and recapitulate the severe HC planar misorientation reported previously (Fig. S2C) (Tarchini et al., 2013). These animals die shortly after birth, however, so we used *Atoh1-Cre* (Matei et al., 2005) to restrict PTXa mostly to post-mitotic HCs in order to study postnatal bundle morphogenesis. *Atoh1-Cre; PTXa* IHCs have bundle defects that are strikingly reminiscent of *Lgn* mutants, with supernumerary rows of identical-looking stereocilia and a drastically shortened first row (Fig. 2B–F). Thus, LGN and *Gai* are both required for postnatal stereocilia elongation and play an essential role in generating graded asymmetric identities across rows, with mutant IHCs harboring an almost flat bundle of ‘generic’ stereocilia. OHC bundle defects are generally similar but less severe, with supernumerary rows largely corrected at maturity and normal stereocilia thickness across rows (Fig. 2B,G–I; data not shown). Milder first row shortening and better preserved staircase-like organization probably reflects the fact that first row elongation and thickening is much less pronounced in OHCs compared with IHCs (compare Fig. 2C,D,G,H). Stereocilia shortening and shallower staircase patterns are also observed in vestibular HCs in the utricle (Fig. S3B–D).

At mature stages, the IHCs of *Atoh1-Cre; PTXa* mutants have longer stereocilia than do *Lgn* mutants (Fig. 2B,C). Milder shortening could reflect a knock-down rather than a full inactivation of *Gai* function by PTXa. Accordingly, leftover *Gai* protein can be detected in less differentiated HCs, where Cre expression occurs later (Fig. S2D). By contrast, disorganized stereocilia distribution at the apical membrane is more pronounced in *Atoh1-Cre; PTXa* than in *Lgn* mutants (Fig. 2J). It will be interesting to combine *Gnai1-Gnai2-Gnai3* mutants to extend the PTXa results by removing single or multiple endogenous *Gai* proteins.

Although loss-of-function approaches cannot resolve subcellular protein function, we propose that the LGN-*Gai* complex regulates stereocilia elongation from their stereocilia tip location because: (1) shorter stereocilia are observed postnatally, when LGN-*Gai* tip enrichment is more prominent and bare zone accumulation decreases; (2) resident proteins are more likely to influence stereocilia elongation than proteins located outside the bundle; and (3) proteins localized at stereocilia tips and regulating height have been reported previously (Manor and Kachar, 2008) (discussed below).

### Stereocilia stunting in absence of LGN-*Gai* coincides with profound hearing loss

Very limited auditory brainstem responses could be elicited from click sounds and pure tone frequencies (8, 16 and 32 kHz) in young *Lgn* and *Atoh1-Cre; PTXa* adult mutants at the highest sound pressure tested (Fig. 3A,B). Stunted stereocilia are a likely cause for near-complete deafness, and could be the etiology of hereditary hearing loss reported in multiple families with recessive mutations in *LGN/GPSM2* (Doherty et al., 2012; Walsh et al., 2010; Yariz et al., 2012). In addition, planar polarity defects and abnormal stereocilia distribution could also play a role (Bhonker et al., 2016; Ezan et al., 2013; Tarchini et al., 2013). Direct binding between LGN and *Gai* is essential for proper bundle morphogenesis and hearing, as suggested by a recent study using a mutant in which LGN lacks the Goloco motifs that mediate its interaction with *Gai* (Bhonker et al., 2016). Of note, *Lgn* and *Atoh1-Cre; PTXa* cochleas are still able to incorporate the FM1-43 dye, and the *Cdh23* protein can still be detected near stereocilia tips in mature *Lgn* mutants, suggesting that LGN-*Gai* do not directly affect mechanosensory channels or tip-links (Fig. S3E,F). Although *Lgn* and *PTXa* mutants do not display obvious balance problems in their cage, their vestibular HC bundle anomalies (Fig. S3B–D) might possibly explain the poor skills observed during free swimming (Movie 1) (Goodyear et al., 2012). Together, these results underscore the importance of LGN-*Gai* signaling for HC function.

### Evidence for a molecular link between the bare zone and stereocilia tips

In mitotic cells, LGN-*Gai*-mediated regulation of spindle orientation depends on their binding partners (Morin and Bellaïche, 2011). For example, LGN can bind *Insc*, a protein that directs vertical epithelial divisions and is typically absent during planar divisions (Konno et al., 2008; Kraut et al., 1996; Postiglione et al., 2011; Poulson and Lechler, 2010; Žigman et al., 2005). We reasoned that binding partners could differentially regulate the trafficking of LGN-*Gai* to distinct HC compartments. Consistently, we noticed increased amounts of LGN and *Gai* before birth at stereocilia tips in absence of *Insc*, which itself accumulates at the bare zone but not at the tips (Fig. 4A–D and Fig. 1B,G). Interestingly, LGN-*Gai* enrichment at the bare zone is conversely reduced in *Insc* mutants (Fig. 4A–D). The same redistribution across compartments is observed in utricular HCs in *Insc* mutants (Fig. 4E). Thus, before birth, *Insc* buffers LGN-*Gai* at the bare zone, limiting protein amount at tips. Similarly, LGN is required to keep *Gai* at the bare zone, thereby preventing an excess amount of *Gai* from accumulating at stereocilia tips and ectopically localizing at their base (Fig. 4F; Fig. S4A). A proper balance of

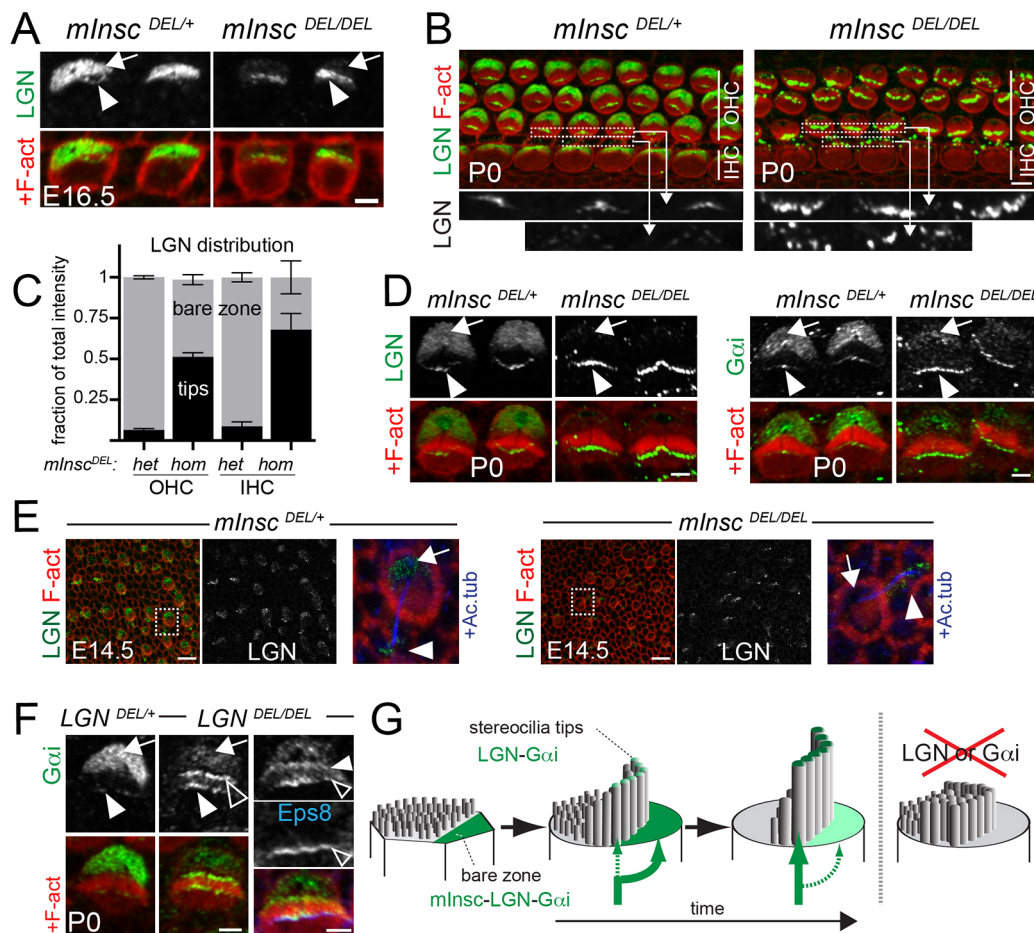


**Fig. 4. Balanced LGN-G $\alpha$ i distribution between the bare zone and stereocilia tips.** (A) LGN immunostaining at E16.5 (apical turn) in the indicated genotypes. Mutant IHCs have decreased levels of LGN at the bare zone (arrow) and increased LGN levels in stereocilia (arrowhead). (B) LGN immunostaining at P0. Boxed regions are shown at higher magnification underneath and specifically show LGN stereocilia enrichment in OHCs and IHCs. (C) Fraction of total LGN staining intensity at the bare zone (gray) and stereocilia tips (black) in OHCs and IHCs of P0 *Insc<sup>DEL/DEL</sup>* and control littermates (mean $\pm$ s.e.m.). Nine OHCs (three per row) and three IHCs at the cochlea base were analyzed for  $n \geq 3$  animals for each genotype. (D) LGN (left) and G $\alpha$ i (right) immunostaining in P0 OHCs. (E) LGN immunostaining in utricular epithelium at E14.5. A single HC (boxed) is magnified in the right-most panels, where acetylated tubulin (Ac. tub) co-staining reveals the kinocilium in blue. (F) G $\alpha$ i immunostaining at P0 in OHCs. G $\alpha$ i excess in the bundle is seen at the tips (solid arrowhead) and the base (open arrowhead) of stereocilia. In the right-most panels, stereocilia tips are labeled with Eps8 (blue). Arrows and arrowheads indicate the bare zone and stereocilia tips, respectively. (G) Model depicting the Insc-LGN-G $\alpha$ i complex distribution (green) during HC differentiation and the mutant phenotype. Scale bars: 2  $\mu$ m in A,D,F; 5  $\mu$ m in B; 10  $\mu$ m in E.

proteins between compartments can be restored by providing Insc or LGN in individual HCs of *Insc* or *Lgn* mutant explants, respectively (Fig. S4B,C). These results uncover a cell-intrinsic mechanism that is able to tune relative protein distribution between compartments. Although this mechanism *de facto* establishes an interesting link between planar polarization and stereocilia tip enrichment in the first row (Fig. 4G), the reason for limiting LGN-G $\alpha$ i amounts at tips before birth is still unclear. LGN-G $\alpha$ i excess at tips in mutants is observed only before the normal increase in protein accumulation there after birth, with unchanged LGN-G $\alpha$ i amounts present at tips postnatally in *Insc* mutant (Fig. S4D). Consistently, transfected Insc no longer antagonizes LGN at tips in more mature *Insc* mutant explants (Fig. S4C). Finally, we did not observe stereocilia over-elongation or obvious bundle defects in *Insc* mutants (not shown). However, transient LGN-G $\alpha$ i excess could produce subtle changes in the kinetics of stereocilia elongation that are difficult to detect in fixed tissue, and LGN-G $\alpha$ i at tips might only influence elongation after birth, when stunted stereocilia start to be visible in the corresponding mutants.

From a top-down perspective, it is tempting to hypothesize that selective trafficking of LGN-G $\alpha$ i into the first row of stereocilia could be achieved through planar polarized enrichment at the bare zone, which is immediately adjacent along the epithelial plane (Fig. 1B; Fig. 4G). Accordingly, LGN-G $\alpha$ i are first enriched at the bare zone before becoming detectable at tips, and bare zone-restricted Insc can influence early accumulation of LGN-G $\alpha$ i at tips. Stereociliary LGN-G $\alpha$ i would then directly define a tallest row identity, and indirectly implement distinct stereocilia heights and girth across rows in the bundle. The tallest row has indeed been shown to influence stereocilia morphology in the shorter rows via tip-links (Caberlotto et al., 2011a,b; Xiong et al., 2012).

Importantly however, further work is required to establish formally a causal link between the planar polarity machinery and staircase architecture in the bundle. As dual LGN-G $\alpha$ i localization is observed throughout HC apical differentiation (E16.5 to P8), time-based conditional genetics is unlikely to help, and alternative approaches will be needed to manipulate protein enrichment in a compartment-specific manner. It will also be interesting to ask

whether LGN-G $\alpha$ i are part of a larger protein complex at stereocilia tips. The Myo15a-Whrn-Eps8 complex is essential for shaping the bundle after birth, and mice with mutations in any of these proteins show stunted stereocilia and shallow staircase organization that is very reminiscent of the LGN-G $\alpha$ i phenotype described here (Manor et al., 2011; Mburu et al., 2003; Probst et al., 1998; Zampini et al., 2011). Interestingly, Myo15a-Whrn-Eps8 are not enriched at the bare zone, or polarized in the plane, and there is currently no explanation for the observation that their graded enrichment at tips is proportional to stereocilia height (Belyantseva et al., 2003, 2005; Delprat et al., 2005; Rzadzinska et al., 2004).

In summary, we report the striking co-occurrence of planar polarity and stereocilia elongation defects in absence of LGN and G $\alpha$ i function. We propose an innovative model whereby planar polarity signals that originate outside the bundle are used to instruct graded stereocilia heights inside the bundle. We identify the Insc-LGN-G $\alpha$ i complex as an outstanding candidate for conveying information across compartments, and establishing the staircase-like bundle architecture that is essential for sensory function in HCs.

## MATERIALS AND METHODS

### Animals

*Lgn* and *Insc* mutants have been described previously (Tarchini et al., 2013). The generation of *PTXa* mice is described in the supplementary Materials and Methods. All animal work was performed in accordance with the Canadian Council on Animal Care guidelines, and reviewed for compliance and approved by the Animal Care and Use Committee of The Jackson Laboratory.

### Immunostaining and FM1-43 uptake

Cochleas and utricles were isolated from the temporal bone and processed for immunostaining as previously described (Tarchini et al., 2013). To compare protein distribution between the bare zone and stereocilia tips (Fig. 4), *Insc* and *Lgn* mutants and control littermates were processed identically and incubated with a pre-pooled mix to ensure similar antibody concentration. The same cochlear position was imaged in controls and mutants using the same exposure settings, and images were treated identically. For FM1-43 uptake, P4 cochleas were immersed in FM1-43FX (ThermoFisher; 5  $\mu$ M) for 1 min, fixed for 10 min in 4% PFA, mounted and imaged immediately. Details of the antibodies used, imaging and quantitative analysis can be found in the supplementary Materials and Methods.

### Cochlear cultures

Briefly, cochleas from CD1 or B6FVB wild-type mice or mutant mice were collected at E14.5, electroporated with 1–5  $\mu$ g/ $\mu$ l circular DNA (27 V, 27 ms, 6 pulses at 500 ms intervals) and cultured for 6 days in Matrigel (Corning), as previously described (Tarchini et al., 2013).

### Scanning electron microscopy

Temporal bones were fixed for 1 h in 4% PFA before exposing the cochlear sensory epithelium and removing the tectorial membrane. Samples were then incubated overnight in 2.5% glutaraldehyde and 4% PFA in 1 mM MgCl<sub>2</sub> and 0.1 M sodium cacodylate buffer. After further dissection, cochlear and utricular samples were progressively dehydrated in ethanol and incubated through a graded isoamyl acetate series, before being dried using critical point drying or hexamethyldisilazane (Electron Microscopy Sciences). After sample sputtering with gold-palladium, images were acquired on a Hitachi 3000N VP at 20 kV using 5000–10,000 $\times$  magnification. Details of the quantitative analysis can be found in the supplementary Materials and Methods.

### Auditory brainstem response and swimming procedure

Briefly, mice were anesthetized with tribromoethanol (2.5 mg per 10 g of body weight), and tested using the Smart EP evoked potential system (Intelligent Hearing Systems) as described previously (Zheng et al., 1999). Thresholds were determined by increasing the sound pressure level (SPL) in

10 dB increments. To observe free swimming behavior (Goodyear et al., 2012), mice were placed in a 38 $\times$ 45 cm plastic tub filled with 10 cm of water at 25°C. Their behavior was filmed for 1 min and videos were evaluated blind to genotype.

### Acknowledgements

We thank Wenning Qin and Yingfan Zhang for technical assistance with the *PTXa* mouse, Cong Tian and Kenneth Johnson for help with Auditory Brainstem Response tests, and Fumio Matsuzaki, Quansheng Du and Jun Yang for LGN and PDZD7 antibodies.

### Competing interests

The authors declare no competing or financial interests.

### Author contributions

Conceptualization: B.T. and M.C.; Experimentation and data analysis: B.T., A.L.D.T. and N.D.; Manuscript writing: B.T.; Manuscript editing: M.C. and A.L.D.T.; Supervision and funding: B.T. and M.C.

### Funding

This work was supported by a research grant from the Canadian Institutes of Health Research [MOP-102584] to M.C. and by a start-up from the Jackson Laboratory to B.T. B.T. was supported by a Human Frontiers Science Program long-term fellowship [LT 00041/2007-L/3] and M.C. is a Senior Fellow of the Fonds de la recherche du Québec–Santé/Fondation Antoine Turmel.

### Supplementary information

Supplementary information available online at <http://dev.biologists.org/lookup/doi/10.1242/dev.139089.supplemental>

### References

- Belyantseva, I. A., Boger, E. T. and Friedman, T. B. (2003). Myosin XVa localizes to the tips of inner ear sensory cell stereocilia and is essential for staircase formation of the hair bundle. *Proc. Natl. Acad. Sci. USA* **100**, 13958–13963.
- Belyantseva, I. A., Boger, E. T., Naz, S., Frolenkov, G. I., Sellers, J. R., Ahmed, Z. M., Griffith, A. J. and Friedman, T. B. (2005). Myosin-XVa is required for tip localization of whirlin and differential elongation of hair-cell stereocilia. *Nat. Cell Biol.* **7**, 148–156.
- Bhonker, Y., Abu-Rayyan, A., Ushakov, K., Amir-Zilberstein, L., Shivatzki, S., Yizhar-Barnea, O., Elkan-Miller, T., Tayeb-Fligelman, E., Kim, S. M., Landau, M. et al. (2016). The GPSM2/LGN GoLoco motifs are essential for hearing. *Mamm. Genome* **27**, 29–46.
- Caberlotto, E., Michel, V., Boutet de Monvel, J. and Petit, C. (2011a). Coupling of the mechanotransduction machinery and stereocilia F-actin polymerization in the cochlear hair bundles. *Bioarchitecture* **1**, 169–174.
- Caberlotto, E., Michel, V., Foucher, I., Bahloul, A., Goodyear, R. J., Pepermans, E., Michalski, N., Perfettini, I., Alegria-Prevot, O., Chardenoux, S. et al. (2011b). Usher type 1G protein sans is a critical component of the tip-link complex, a structure controlling actin polymerization in stereocilia. *Proc. Natl. Acad. Sci. USA* **108**, 5825–5830.
- Delprat, B., Michel, V., Goodyear, R., Yamasaki, Y., Michalski, N., El-Amraoui, A., Perfettini, I., Legrain, P., Richardson, G., Hardelin, J. P. et al. (2005). Myosin XVa and whirlin, two deafness gene products required for hair bundle growth, are located at the stereocilia tips and interact directly. *Hum. Mol. Genet.* **14**, 401–410.
- Doherty, D., Chudley, A. E., Coghlan, G., Ishak, G. E., Innes, A. M., Lemire, E. G., Rogers, R. C., Mhanni, A. A., Phelps, I. G., Jones, S. J. M. et al. (2012). GPSM2 mutations cause the brain malformations and hearing loss in Chudley-McCullough syndrome. *Am. J. Hum. Genet.* **90**, 1088–1093.
- Du, Q. and Macara, I. G. (2004). Mammalian Pins is a conformational switch that links NuMA to heterotrimeric G proteins. *Cell* **119**, 503–516.
- Ebrahim, S., Avenarius, M. R., Grati, M., Krey, J. F., Windsor, A. M., Sousa, A. D., Ballesteros, A., Cui, R., Millis, B. A., Salles, F. T. et al. (2016). Stereocilia-staircase spacing is influenced by myosin III motors and their cargos espin-1 and espin-like. *Nat. Commun.* **7**, 10833.
- Ezan, J., Lasvaux, L., Gezer, A., Novakovic, A., May-Simera, H., Belotti, E., Lhoumeau, A.-C., Birnbaumer, L., Beer-Hammer, S., Borg, J. P. et al. (2013). Primary cilium migration depends on G-protein signalling control of subapical cytoskeleton. *Nat. Cell Biol.* **15**, 1107–1115.
- Goodyear, R. J., Jones, S. M., Sharifi, L., Forge, A. and Richardson, G. P. (2012). Hair bundle defects and loss of function in the vestibular end organs of mice lacking the receptor-like inositol lipid phosphatase PTPRQ. *J. Neurosci.* **32**, 2762–2772.

- Grimsley-Myers, C. M., Sipe, C. W., Geleoc, G. S. G. and Lu, X.** (2009). The small GTPase Rac1 regulates auditory hair cell morphogenesis. *J. Neurosci.* **29**, 15859-15869.
- Hébert, J. M. and McConnell, S. K.** (2000). Targeting of cre to the Foxg1 (BF-1) locus mediates loxP recombination in the telencephalon and other developing head structures. *Dev. Biol.* **222**, 296-306.
- Jones, C., Roper, V. C., Foucher, I., Qian, D., Banizs, B., Petit, C., Yoder, B. K. and Chen, P.** (2008). Ciliary proteins link basal body polarization to planar cell polarity regulation. *Nat. Genet.* **40**, 69-77.
- Konno, D., Shioi, G., Shitamukai, A., Mori, A., Kiyonari, H., Miyata, T. and Matsuzaki, F.** (2008). Neuroepithelial progenitors undergo LGN-dependent planar divisions to maintain self-renewability during mammalian neurogenesis. *Nat. Cell Biol.* **10**, 93-101.
- Kraut, R., Chia, W., Jan, L. Y., Jan, Y. N. and Knoblich, J. A.** (1996). Role of inscuteable in orienting asymmetric cell divisions in *Drosophila*. *Nature* **383**, 50-55.
- Lelli, A., Michel, V., Boutet de Monvel, J., Cortese, M., Bosch-Grau, M., Aghaie, A., Perfettini, I., Dupont, T., Avan, P., El-Amraoui, A. et al.** (2016). Class III myosins shape the auditory hair bundles by limiting microvilli and stereocilia growth. *J. Cell Biol.* **212**, 231-244.
- Manor, U. and Kachar, B.** (2008). Dynamic length regulation of sensory stereocilia. *Semin. Cell Dev. Biol.* **19**, 502-510.
- Manor, U., Disanza, A., Grati, M. H., Andrade, L., Lin, H., Di Fiore, P. P., Scita, G. and Kachar, B.** (2011). Regulation of stereocilia length by myosin XVa and whirlin depends on the actin-regulatory protein Eps8. *Curr. Biol.* **21**, 167-172.
- Matei, V., Pauley, S., Kaing, S., Rowitch, D., Beisel, K. W., Morris, K., Feng, F., Jones, K., Lee, J. and Fritsch, B.** (2005). Smaller inner ear sensory epithelia in Neurog1 null mice are related to earlier hair cell cycle exit. *Dev. Dyn.* **234**, 633-650.
- May-Simera, H. and Kelley, M. W.** (2012). Planar cell polarity in the inner ear. *Curr. Top. Dev. Biol.* **101**, 111-140.
- Mburu, P., Mustapha, M., Varela, A., Weil, D., El-Amraoui, A., Holme, R. H., Rump, A., Hardisty, R. E., Blanchard, S., Coimbra, R. S. et al.** (2003). Defects in whirlin, a PDZ domain molecule involved in stereocilia elongation, cause deafness in the whirler mouse and families with DFNB31. *Nat. Genet.* **34**, 421-428.
- Milligan, G.** (1988). Techniques used in the identification and analysis of function of pertussis toxin-sensitive guanine nucleotide binding proteins. *Biochem. J.* **255**, 1-13.
- Morin, X. and Bellaïche, Y.** (2011). Mitotic spindle orientation in asymmetric and symmetric cell divisions during animal development. *Dev. Cell* **21**, 102-119.
- Pickles, J. O., Comis, S. D. and Osborne, M. P.** (1984). Cross-links between stereocilia in the guinea pig organ of Corti, and their possible relation to sensory transduction. *Hear. Res.* **15**, 103-112.
- Postiglione, M. P., Jüschke, C., Xie, Y., Haas, G. A., Charalambous, C. and Knoblich, J. A.** (2011). Mouse inscuteable induces apical-basal spindle orientation to facilitate intermediate progenitor generation in the developing neocortex. *Neuron* **72**, 269-284.
- Poulson, N. D. and Lechler, T.** (2010). Robust control of mitotic spindle orientation in the developing epidermis. *J. Cell Biol.* **191**, 915-922.
- Probst, F. J., Fridell, R. A., Raphael, Y., Saunders, T. L., Wang, A., Liang, Y., Morell, R. J., Touchman, J. W., Lyons, R. H., Noben-Trauth, K. et al.** (1998). Correction of deafness in shaker-2 mice by an unconventional myosin in a BAC transgene. *Science* **280**, 1444-1447.
- Rzadzinska, A. K., Schneider, M. E., Davies, C., Riordan, G. P. and Kachar, B.** (2004). An actin molecular treadmill and myosins maintain stereocilia functional architecture and self-renewal. *J. Cell Biol.* **164**, 887-897.
- Salles, F. T., Merritt, R. C., Jr., Manor, U., Dougherty, G. W., Sousa, A. D., Moore, J. E., Yengo, C. M., Dosé, A. C. and Kachar, B.** (2009). Myosin IIIa boosts elongation of stereocilia by transporting espin 1 to the plus ends of actin filaments. *Nat. Cell Biol.* **11**, 443-450.
- Shotwell, S. L., Jacobs, R. and Hudspeth, A. J.** (1981). Directional sensitivity of individual vertebrate hair cells to controlled deflection of their hair bundles. *Ann. N. Y. Acad. Sci.* **374**, 1-10.
- Sipe, C. W. and Lu, X.** (2011). Kif3a regulates planar polarization of auditory hair cells through both ciliary and non-ciliary mechanisms. *Development* **138**, 3441-3449.
- Tarchini, B., Jolicoeur, C. and Cayouette, M.** (2013). A molecular blueprint at the apical surface establishes planar asymmetry in cochlear hair cells. *Dev. Cell* **27**, 88-102.
- Walsh, T., Shahin, H., Elkan-Miller, T., Lee, M. K., Thornton, A. M., Roeb, W., Abu Rayyan, A., Loulus, S., Avraham, K. B., King, M. C. et al.** (2010). Whole exome sequencing and homozygosity mapping identify mutation in the cell polarity protein GPSM2 as the cause of nonsyndromic hearing loss DFNB82. *Am. J. Hum. Genet.* **87**, 90-94.
- Wise, A., Watson-Koken, M.-A., Rees, S., Lee, M. and Milligan, G.** (1997). Interactions of the alpha2A-adrenoceptor with multiple Gi-family G-proteins: studies with pertussis toxin-resistant G-protein mutants. *Biochem. J.* **321**, 721-728.
- Xiong, W., Grillet, N., Elledge, H. M., Wagner, T. F. J., Zhao, B., Johnson, K. R., Kazmierczak, P. and Müller, U.** (2012). TMHS is an integral component of the mechanotransduction machinery of cochlear hair cells. *Cell* **151**, 1283-1295.
- Yariz, K. O., Walsh, T., Akay, H., Duman, D., Akkaynak, A. C., King, M.-C. and Tekin, M.** (2012). A truncating mutation in GPSM2 is associated with recessive non-syndromic hearing loss. *Clin. Genet.* **81**, 289-293.
- Zampini, V., Rüttiger, L., Johnson, S. L., Franz, C., Furness, D. N., Waldhaus, J., Xiong, H., Hackney, C. M., Holley, M. C., Offenhauser, N. et al.** (2011). Eps8 regulates hair bundle length and functional maturation of mammalian auditory hair cells. *PLoS Biol.* **9**, e1001048.
- Zhao, B. and Müller, U.** (2015). The elusive mechanotransduction machinery of hair cells. *Curr. Opin. Neurobiol.* **34**, 172-179.
- Zheng, Q. Y., Johnson, K. R. and Erway, L. C.** (1999). Assessment of hearing in 80 inbred strains of mice by ABR threshold analyses. *Hear. Res.* **130**, 94-107.
- Žigman, M., Cayouette, M., Charalambous, C., Schleiffer, A., Hoeller, O., Dunican, D., McCudden, C. R., Firnberg, N., Barres, B. A., Siderovski, D. P. et al.** (2005). Mammalian inscuteable regulates spindle orientation and cell fate in the developing retina. *Neuron* **48**, 539-545.